Penerbit Akademia Baru

CFD Letters

Journal homepage: www.akademiabaru.com/cfdl.html
ISSN: 2180-1363

The Effect of Triangular Cavity Shape on the Hybrid Microchannel Heat Sink Performance

Open Access

Wan Mohd. Arif Aziz Japar[1,*], Nor Azwadi Che Sidik[1], R. Saidur[2], Natrah Kamaruzaman[3], Yutaka Asako[1], Siti Nurul Akmal Yusof[1]

[1] Malaysian-Japan International Institute of Technology, Universiti Teknologi Malaysia, 54100 Kuala Lumpur, Wilayah Persekutuan Kuala Lumpur, Malaysia
[2] Research Centre for Nano-Materials and Energy Technology, School of Science and Technology, Sunway University, Bandar Sunway, 47500 Subang Jaya, Selangor, Malaysia
[3] Department of Thermofluid, School of Mechanical Engineering, Faculty of Engineering, Universiti Teknologi Malaysia, 81310 Skudai, Johor, Malaysia

ARTICLE INFO

Article history:
Received 22 July 2020
Received in revised form 20 September 2020
Accepted 23 September 2020
Available online 29 September 2020

ABSTRACT

Rapid development in the electronic industry witnesses many tremendous advanced technologies which work with high power density. As a result, an advanced cooling technique, namely, microchannel heat sink (MCHS) is required to fulfil the current cooling demand due to unpredicted increment of power density in a high-density microchip. A microchannel heat sink performance can be enhanced by improving the working fluid properties and or improving the design of cooling passage that contributes to the augmentation of heat transfer rate. In this paper, the optimization of hydrothermal performance was conducted by studying the effect of triangular cavity pitch location (Cavity 1, CV1: 60 µm; Cavity 2, CV2: 100 µm; Cavity 3, CV3: 140 µm) on fluid flow and heat transfer characteristic in the hybrid microchannel heat sink (Triangular cavity with rectangular rib microchannel heat sink, TC-RR MCHS). The result revealed that the TC-RR MCHS with the triangular cavity pitch location of 140 µm (CV3) showed superior performance over other pitch locations (CV1 and CV2) for all the Reynolds number (Re number). The optimum Performance Factor, PF, achieved by CV3 pitch location was 1.76 at Re number of 350. It indicates that the proposed design with CV3 is suitable for the technology that requires less pumping power consumption.

Keywords:
Thermal management; Convective heat transfer; Hybrid microchannel heat sink; Triangular cavity; Performance factor; Pumping power

Copyright © 2020 PENERBIT AKADEMIA BARU - All rights reserved

1. Introduction

Nowadays, demand for the high-performance electronic device that easies for handling and comfortable to carry everywhere has changed the trend of electronic industry for developing new technology with the miniaturization of mechanical structures and electronic component. This

* *Corresponding author.*
E-mail address: arifklang@gmail.com (Wan Mohd. Arif Aziz Japar)

https://doi.org/10.37934/cfdl.12.9.114

condition increases the heat flux dissipation due to the unpredicted augmentation of power density carried by the compact electronic device. The reliability of an electronic device drops up to half of its original value if the temperature of the electronic device rises 10°C sharply. If the temperature of an electronic device increases from 77°C – 125°C, the reliability of the electronic device reduces by 20% of its original value [1]. Therefore, an efficient cooling method needs to be developed to control the operating temperature so that the temperature does not go beyond the junction temperature [2].

There have some advance techniques have been studied by former researchers in micro-cooling method, namely, microchannel heat sink, micro-jet impingement, micro heat pipe and micro electro hydrodynamic. Among these methods, microchannel heat sink appears as a promising method which can provide high heat transfer rate in a cooling system [3]. It was proved by the Tuckerman and Pease [3] in 1981. However, for the current electronic device, the conventional design which has straight channels restrains the performance of microchannel heat sink as a cooling device due to boundary layer thickness that created by laminar region in the channels. The boundary layer thickness increases the thermal resistance and thus reduce the heat transfer performance. Since then, many researchers tried to improve the performance of the microchannel heat sink by using the active and passive method [4].

In recent year, many researchers [5-7] focused on the passive method to improve the performance of microchannel heat sink due to no external energy and moving part in the cooling device. Generally, there have two techniques in passive method to improve cooling performance such as improve the working fluid properties [8, 9] or improve the design of cooling passage [10, 11] which contributes to the enhancement of heat transfer rate. Cavity geometry is one of the passive methods that has been used by previous researchers in enhanced MCHS design. The cavity geometry is used to reduce surface roughness and pressure drop penalty by providing a large flow area in the channel of MCHS. This method is very useful in hybrid passive MCHS than in single passive technique [12, 13]. In 2016, Li *et al.,* [13] studied the combined effect of cavity and rib in hybrid designs. The study revealed that the hybrid technique obtained a remarkable heat transfer performance enhancement with an acceptable pressure drop penalty compared to the single passive method of cavity MCHS. This analysis is supported by Ghani *et al.,* [12]'s novel work which has a similar design but with a different shape of cavity geometry. For more understanding about the potential of cavity geometry, Li *et al.,* [14] extended his work by evaluating the effect of cavity shape on hydrothermal performance. The analysis illustrated that a boundary-layer interruption and local fluid disturbance which provided by triangular cavity geometry was very aggressive than fan-shaped cavity and trapezoid cavity. However, a vortex dead zone in the triangular cavity corner increased the residence time of fluid in the cavity which weakened the heat transfer performance in the cavity area.

In 2018, Japar and his team [15] tried to suppress the vortex dead zone by introducing secondary channel in between triangular cavity geometry of adjacent main channel. The work illustrated that the presence of secondary channels eliminated the vortex dead zone and thus improved the heat transfer performance in the cavity area. Besides that, the combination of the cavity and secondary channel geometry also enhanced the overall performance of the microchannel heat sink. After a year, Japar *et al.,* [16] extended his research in order to improve the economic management of cavity-rib MCHS via a secondary channel geometry. The study revealed that the combination of the sinusoidal cavity with rib and secondary channel increased the overall performance of microchannel heat sink at low range Re number, which contributed to the less pumping power consumption.

Throughout all the studies reviewed here, the cavity geometry is recognized as one of passive method that can improve both the thermal and economic management. But it only can be obtained by hybrid passive technique. Those studies presented thus far provide evidence that cavity shape gives a significant effect on fluid flow and heat transfer characteristic. A triangular cavity shape gives

a substantial impact on the fluid-structure due to the more massive vortex flows that generated in a hybrid MCHS. However, a vortex dead zone in the cavity corner increase the residence time of fluid in that area and thus reduce the efficiency of heat transfer.

As a consequence, the overall performance of the hybrid microchannel heat sink decreases at the higher Re number due to the weak heat transfer performance is dominated by the generated pressure drop. To the best of authors' knowledge, there has no study that analyses the effect of triangular cavity shape on hydrothermal performance. In this paper, a hybrid MCHS with three different shapes of the triangular cavity (Cavity 1, CV1: 60 µm; Cavity 2, CV2: 100 µm; Cavity 3, CV3: 140 µm) are investigated in order to find the optimum triangular cavity geometry parameter which can provide high overall performance at low Re number which could prevent a high-pressure drop in the hybrid MCHS.

2. Methodology

This hybrid microchannel heat sink is made by a copper and consist of ten microchannels. However, in order to save the computational cost, only one symmetrical part of the microchannel heat sink is adopted in the present simulation, as shown in Figure 1(a). Table 1 shows the parameter description for the geometry illustrated in Figure 1(b).

Figure 2 shows the three different shapes of TC-RR MCHS triangular cavity that will be analyzed in this paper. The shape of CV1, CV2 and CV3 designs are dependent on the location of pitch cavity (L1) which parallel to the channel axis. The pitch of CV1, CV2 and CV3 that measured from the leading edge of the cavity are 60 µm, 100 µm and 140 µm, respectively. The shape of the cavity will change a flow structure in the hybrid microchannel and affect the heat transfer performance, friction loss and overall performance of the microchannel heat sink.

Table 1
Geometry parameters of TC-RR MCHS

Parameter	Value
Lt	10,000 µm
Wt	200 µm
Ht	350 µm
Hc	200 µm
Wc	100 µm
Lr	60 µm
Wr	30 µm
La	400 µm
L1 & L2 (Three different shapes)	CV1: L1: 60 µm L2: 140 µm CV2: L1: 100 µm L2: 100 µm CV3: L1: 140 µm L2: 60 µm
L3	200 µm
Wtc	112 µm

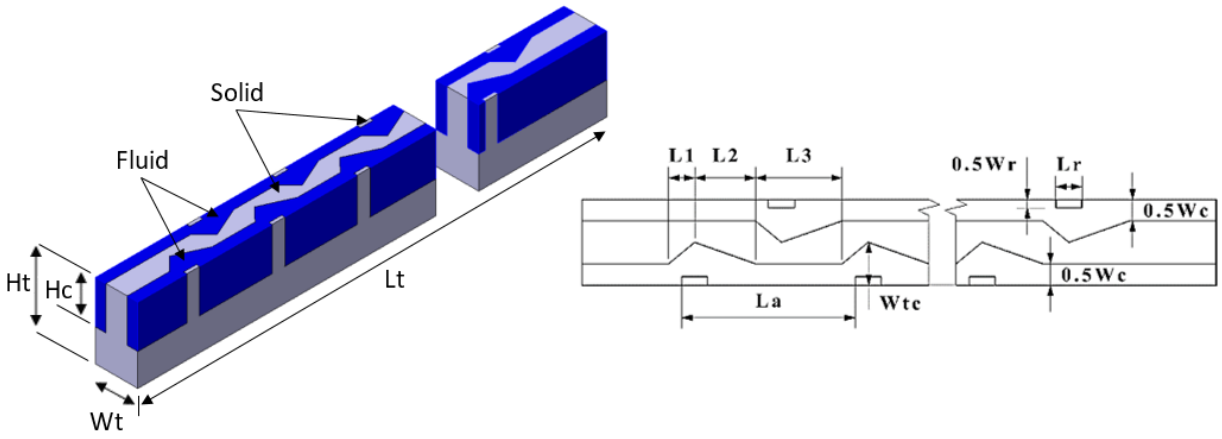

(a) (b)

Fig. 1. TC-RR MCHS (a) One symmetrical part (b) Geometry parameter

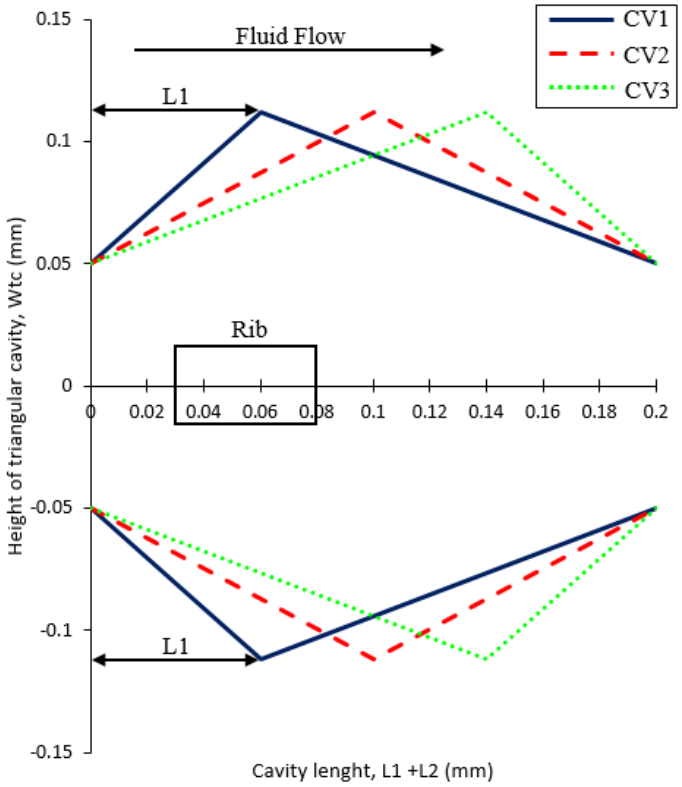

Fig. 2. Triangular cavity with the three different shapes

2.1 Governing Equation

In the current analysis, prediction of fluid flow, heat and mass transfer in all three-dimensional geometry designs are numerically solved by the set of governing mathematical equations, namely, conservation of mass, conservation of momentum and conservation of energy, in ANSYS FLUENT 17.0. Finite volume method is utilized to discretize the governing equation. The SIMPLE algorithm was adopted to accomplish the pressure-velocity coupling. At the same time, the second-order upwind scheme is used for the convective term, and second-order central difference scheme is applied for the diffusion term. Furthermore, convergence criteria are set to be less than 10^{-6} for continuity and less than 10^{-9} for energy. The governing equations are solved according to the following assumptions:

I. Fluid in this study is water. The fluid is incompressible and Newtonian.
II. Knudsen number, Kn of water in microfluidic channels is less than 10^{-3}. The fluid flow can be assumed as a continuum. At this condition, the non-slip boundary condition and Navier-stokes equation are applicable.
III. The flow condition is laminar.
IV. Both the fluid flow and heat transfer process is in a steady-state condition.
V. Gravitational force, viscous dissipation and radiation heat transfer are neglected.
VI. Thermophysical properties of water are constant.

After considering these assumptions, the governing mathematical equations are written as follow:

Continuity equation:

$$\frac{\partial u}{\partial x}+\frac{\partial v}{\partial y}+\frac{\partial w}{\partial z}=0 \tag{1}$$

velocity components in x, y and z-directions are labelled as u, v and w, respectively.

Momentum equations:

$$u\frac{\partial u}{\partial x}+v\frac{\partial u}{\partial y}+w\frac{\partial u}{\partial z}=-\frac{1}{\rho_f}\frac{\partial p}{\partial x}+\frac{\mu_f}{\rho_f}\left(\frac{\partial^2 u}{\partial x^2}+\frac{\partial^2 u}{\partial y^2}+\frac{\partial^2 u}{\partial z^2}\right) \tag{2}$$

$$u\frac{\partial v}{\partial x}+v\frac{\partial v}{\partial y}+w\frac{\partial v}{\partial z}=-\frac{1}{\rho_f}\frac{\partial p}{\partial y}+\frac{\mu_f}{\rho_f}\left(\frac{\partial^2 v}{\partial x^2}+\frac{\partial^2 v}{\partial y^2}+\frac{\partial^2 v}{\partial z^2}\right) \tag{3}$$

$$u\frac{\partial w}{\partial x}+v\frac{\partial w}{\partial y}+w\frac{\partial w}{\partial z}=-\frac{1}{\rho_f}\frac{\partial p}{\partial z}+\frac{\mu_f}{\rho_f}\left(\frac{\partial^2 w}{\partial x^2}+\frac{\partial^2 w}{\partial y^2}+\frac{\partial^2 w}{\partial z^2}\right) \tag{4}$$

density, dynamic viscosity and pressure of coolant are labelled as ρ_f, μ_f and p, respectively.

Energy equation of coolant and solid region are shown below:

$$u\frac{\partial T_f}{\partial x}+v\frac{\partial T_f}{\partial y}+w\frac{\partial T_f}{\partial z}=\frac{k_f}{\rho_f c_{Pf}}\left(\frac{\partial^2 T_f}{\partial x^2}+\frac{\partial^2 T_f}{\partial y^2}+\frac{\partial^2 T_f}{\partial z^2}\right) \tag{5}$$

$$0=k_s\left(\frac{\partial^2 T_s}{\partial x^2}+\frac{\partial^2 T_s}{\partial y^2}+\frac{\partial^2 T_s}{\partial z^2}\right) \tag{6}$$

Parameters that involved in these equations are fluid temperature, T_f solid temperature, T_s fluid thermal conductivity, k_f solid thermal conductivity, k_s and heat capacity, c_{Pf}.

Penerbit Akademia Baru

2.2 Boundary Condition

Two boundary conditions were set in the simulation analysis, namely, hydrodynamic boundary condition and thermal boundary condition. The details for both conditions are shown in Table 2.

Table 2
The boundary condition for simulation analysis

Boundary	Location	Condition
Hydrodynamic	At the fluid-solid interface	No-slip and no penetration $u = v = w = 0$ $-k_s(\frac{\partial T_s}{\partial n}) = -k_f(\frac{\partial T_f}{\partial n})$ where n is the coordinate normal to the wall
	At inlet, $x = 0$	$u_f = u_{in}$ $x = L_t = 10mm$
	At outlet, $x = L_t = 10mm$	$p_f = p_{out} = 1\ atm$
Thermal	At inlet, $x = 0$	$T_f = T_{in} = 300K$ (for water) $-k_s(\frac{\partial T_s}{\partial x}) = 0$ (for solid)
	At outlet, $x = L_t = 10mm$	$-k_f(\frac{\partial T_f}{\partial x}) = 0$ (for water) $-k_s(\frac{\partial T_s}{\partial x}) = 0$ (for solid)
	At the top wall, $z = Ht = 0.35mm$	$u = v = w = 0$ $-k_s(\frac{\partial T_s}{\partial z}) = 0$
	At the bottom wall, $z = 0$	$-k_s(\frac{\partial T_s}{\partial z}) = q_w = 100W/cm^2$
	At the sidewall, $y = 0$	$\frac{\partial}{\partial y} = 0$ (symmetry)
	At the sidewall, $y = Wt = 0.2mm$	$\frac{\partial}{\partial y} = 0$ (symmetry)

2.3 Data Acquisition

The average convective heat transfer coefficient and the average Nusselt number are calculated by Eq. (7) and Eq. (8), respectively.

$$h_{ave} = \frac{q_w A_{film}}{A_{con.}(T_{W,ave} - T_{f,ave})} \tag{7}$$

$$Nu_{ave} = \frac{h_{ave} D_h}{k_f} \tag{8}$$

where $T_{f,ave}$, $T_{W,ave}$, A_{film}, $A_{cond.}$ and q_w are average fluid temperature, average wall temperature, heated area, convective heat transfer area and the heat flux, respectively.

The dimensionless number, such as Reynold number, hydraulic diameter, D_h and average apparent friction factor, $f_{app,ave}$ is calculated by Eq. (9), Eq. (10) and Eq. (11), respectively.

$$\mathrm{Re} = \frac{\rho u_m D_h}{\mu} \tag{9}$$

$$D_h = \frac{2H_c W_c}{H_c + W_c} \tag{10}$$

$$f_{app,ave} = \frac{2D_h \Delta P}{Lt \rho u_m^2} \tag{11}$$

Microchannel total length and pressure drop are labelled as Lt and ΔP, respectively.

2.4 Performance Factor

The overall performance of enhanced microchannel heat sink designs is evaluated by performance factor, Pf. This analysis is conducted in order to find the best triangular cavity shape that could provide optimum hydrothermal performance at the lower range of Re number. Performance factor is an indicator to identify which designs could give a significant impact on heat transfer performance with minimal pressure drop penalty. This performance factor can be expressed as:

$$Pf = \frac{Nu/Nu_o}{(f/f_o)^{(1/3)}} \tag{12}$$

Nusselt number ratio, (Nu/Nu_o) and friction factor ratio, (f/f_o) are measured by comparing the enhanced microchannel heat sink designs with the reference/conventional design such as straight rectangular microchannel heat sink (CR MCHS) which labelled by the subscript (o). If the value of Pf is greater than 1, means that, the enhancement of heat transfer performance that obtained by enhanced designs dominates the pressure drop penalty that generated in their channel. While the condition is vice versa for the Pf is lower than 1.

3. Result and Discussion

Before analysing the enhanced microchannel heat sink, the CR MCHS was validated first with the previous study [17, 18]. The deviation error between the simulation result and the previous studies was controlled less than 10% [19-21]. Next, a grid independency test was conducted in order to find the optimum mesh structure that can provide an accurate result with minimal time and computational cost. Besides that, this test aims to eliminate the effect of grid size on simulation results.

3.1 Validation and Grid Independence Test

The validation process was conducted in order to check the accuracy of the simulation model. Parameters that have been chosen as references in the validation process were Local Nusselt number, Nu_x and Average Friction Factor, $f_{app,Ave}$. These two parameters were compared with correlations established by Philips [17] and Shah & London [18]. Figure 3 shows that the highest deviation obtained by Nu_x and $f_{app,Ave}$ are 6.7% and 3.9%, respectively. The results prove that the simulation model has an excellent agreement with the selected previous study. Meaning that the grid number of mesh that utilized in the reference design (Grid number: 5.0×10^5) can be adopted in the enhanced microchannel heat sink.

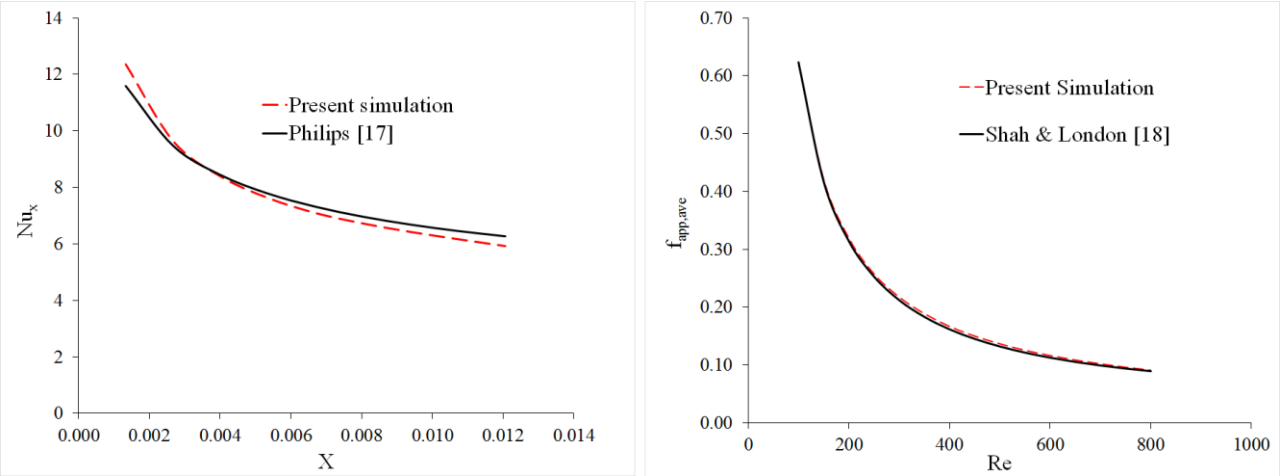

Fig. 3. Simulation model validation with the established correlation of Philips [17] and Shah & London [18] for Local Nusselt number and Average Friction Factor

However, in order to save computational cost and time, a grid independency test was conducted. The finest grid number of 5.0×10^5 was selected as a reference grid in this study. By reducing the grid number, relative error of Nusselt number and pressure drop between the reduced grid number with the finest grid number was calculated and presented in Table 3. Table 3 illustrates the relative error of the Nu number by coarser grids is 0%. However, the pressure drop by the coarser grids varies from the finest grid. The maximum relative error obtained by the coarser grid is 0.20%. In order to control the accuracy of the simulation model, the grid number of $3.0\times10^{5,}$ which has a relative error less than 0.10% was selected and adopted in further analysis for the enhanced microchannel heat sink.

Table 3
Grid independency test

Grid number ($\times10^5$)	Nu	e%	Pressure drop (Pa)	e%
5.0	8.07	-	64599.66	-
4.0	8.07	0%	64574.90	0.038%
3.5	8.07	0%	64557.65	0.065%
3.0	8.07	0%	64535.46	0.099%
2.5	8.07	0%	64507.85	0.142%
2.0	8.07	0%	64480.42	0.185%
1.5	8.07	0%	64465.21	0.200%

3.2 Performance Analysis

In this analysis, two characteristics are considered to evaluate the overall performance of enhanced microchannel heat sink, namely, friction factor ratio, (f/f_o) and Nusselt number ratio, (Nu/Nu_o) as shown in Figure 4 and Figure 6, respectively. Figure 4 shows that friction factor ratio, (f/f_o) of all designs, increase with Re number. At the lower Re number, friction factor ratio, (f/f_o) of all designs are quite similar. However, the friction factor ratio, (f/f_o) of CV3 design increases rapidly compared to CV1 and CV2 designs when the Re number increases further. Among all the designs, CV1 design shows the lowest friction factor ratio, (f/f_o) compared to CV2 and CV3 designs.

Figure 5 illustrates the velocity contour and streamlines distribution for the Re number of 100 and 350. At Re = 100, the friction factor ratio, (f/f_o) of CV3 design exhibit little bit higher than CV1 and CV2 designs due to the small flow area at the cavity entrance compared to the other designs. When the Re number increases up to 350, CV3 design shows the higher enhancement of friction factor ratio, (f/f_o) compared to CV1 and CV2 designs due to the parallel vortex flows that happens in the CV3 design. In contrast to CV1 and CV2 designs, a vortex flow also shows up at the downstream of rib geometry in CV3 design. Both the vortex flows appear at the parallel condition which perpendicular to the main flow. The vortex flows reduce the flow area of the mainstream, which increase the friction factor ratio, (f/f_o) in the CV3 design due to the enhancement of pressure drop. By considering the economic viewpoint, CV1 design appears as the best design that uses less pumping power consumption compared to CV1 and CV3 designs.

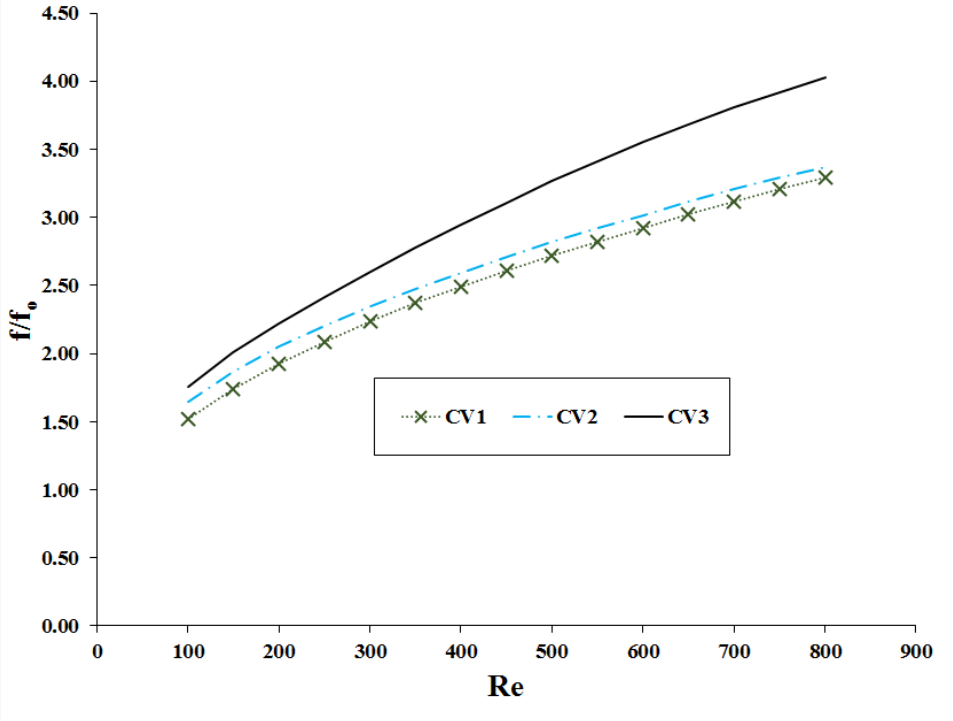

Fig. 4. Friction factor ratio, (f/f_o) of all designs for the Re number of 100 to 800

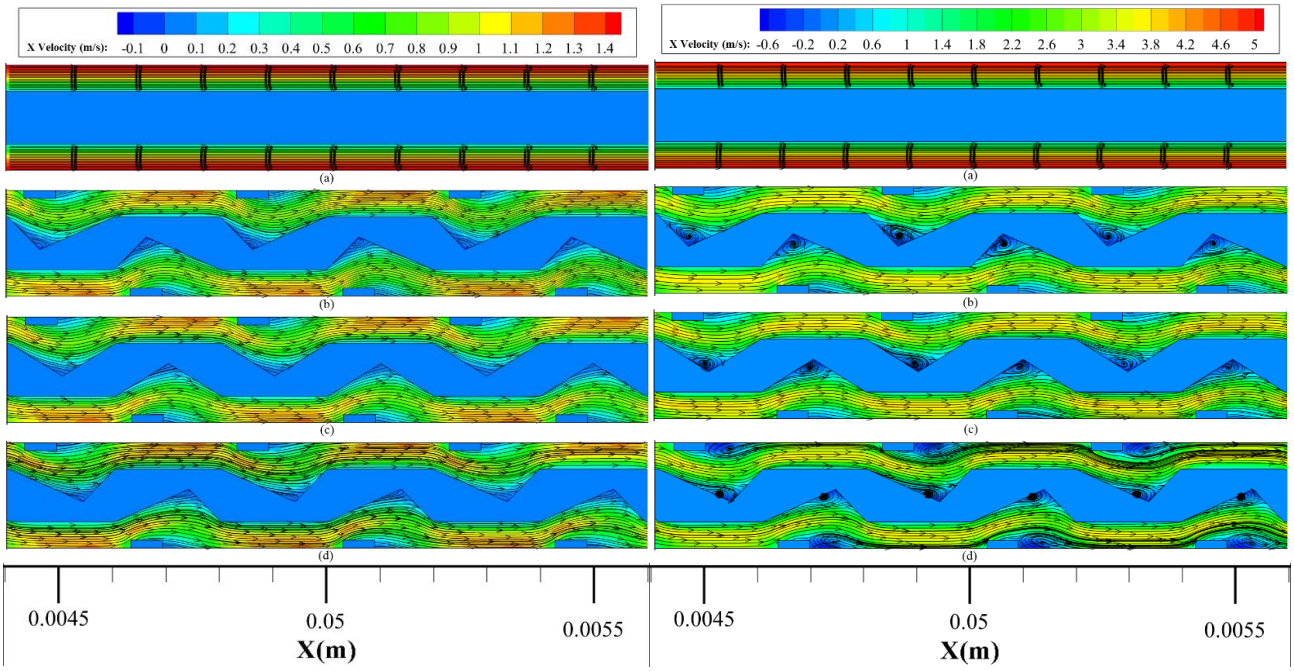

Fig. 5. Velocity contour and streamlines distribution for Re number of 100 (left) and 350 (right) on x-y plane at z = 0.25mm (a) Conventional channel design (CR MCHS) (b) Cavity 1 channel design, CV1 (c) Cavity 2 channel design, CV2 (d) Cavity 3 channel design, CV3

In Figure 6, the effect of cavity geometry shape on heat transfer characteristic is illustrated in Nusselt number ratio, (Nu/Nu_o) form. The figure demonstrates that heat transfer performance of CV2 and CV3 designs increase dramatically at 100≤Re≤400 number, especially in CV3 design. However, at Re>400, the heat transfer performance of CV2 and CV3 designs slowly increase before it reaches their optimum heat transfer performance. As shown in the figure, Nusselt number ratio, (Nu/Nu_o) of CV3 design shows a superior heat transfer performance against all designs for all Re number. In order to demonstrate the superior heat transfer performance that obtained by CV3 design, temperature distribution analysis for Re number of 350 on the x-y plane at z = 0.25mm is conducted as presented in Figure 8. The figure shows that temperature distribution at the sidewall of CV3 design is lower than CV1 and CV2 designs. Besides that, the temperature distribution in the fluid region of CV3 design is more uniform compared to the other designs due to low thermal resistance. As shown in Figure 5, the parallel vortex flows in CV3 design redevelops the boundary layer aggressively compared to the other designs and changes the flow structure from parallel boundary layer as illustrated in CR MCHS to chaotic boundary layer as illustrated in CV3 design which contributes to the more reduction of thermal resistance. For thermal management, CV3 design is the best design compared to the other designs.

Nowadays, both thermal and economic management is essential in the invention and innovation of technology. Also, in this study, both characteristics are considered in order to find an optimum design which can provide a high heat transfer performance with the minimal pressure drop that contributes to the less pumping power consumption compared to CR MCHS. Performance factor, Pf is one of indicator for overall performance evaluation. Figure 7 presents Performance factor, Pf of all designs for the Re number of 100 to 800. The figure demonstrates that Pf of all the designs are higher than one. Means that the designs have a better overall performance than CR MCHS. Among all the designs, CV3 design shows the highest Pf for all the Re number. It achieves the optimum Pf (1.76) at low Re number (Re = 350) whereby it is useful for low pumping power consumption

application. However, when the Re number increases further, the Pf drop slowly due to the rapid growth of friction factor ratio, (f/f_o) at the higher Re number and dominates the heat transfer performance obtained by CV3 design. Means that, simply increase the Re number to achieve the highest performance is not the best method, in fact it increases the pumping power consumption.

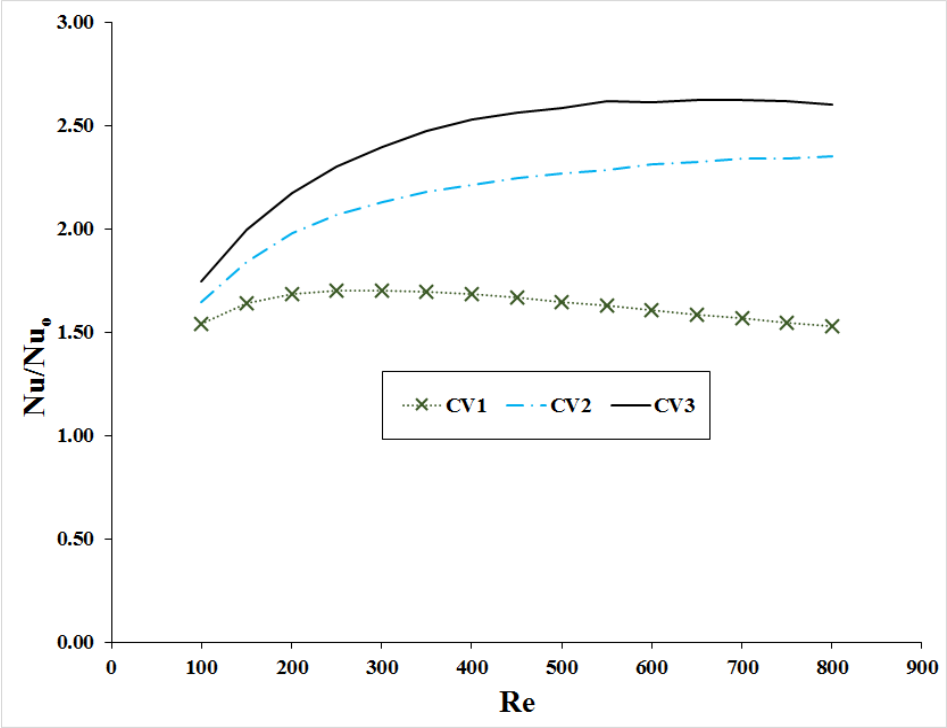

Fig. 6. Nusselt number ratio, (Nu/Nu_o) of all designs for the Re number of 100 to 800

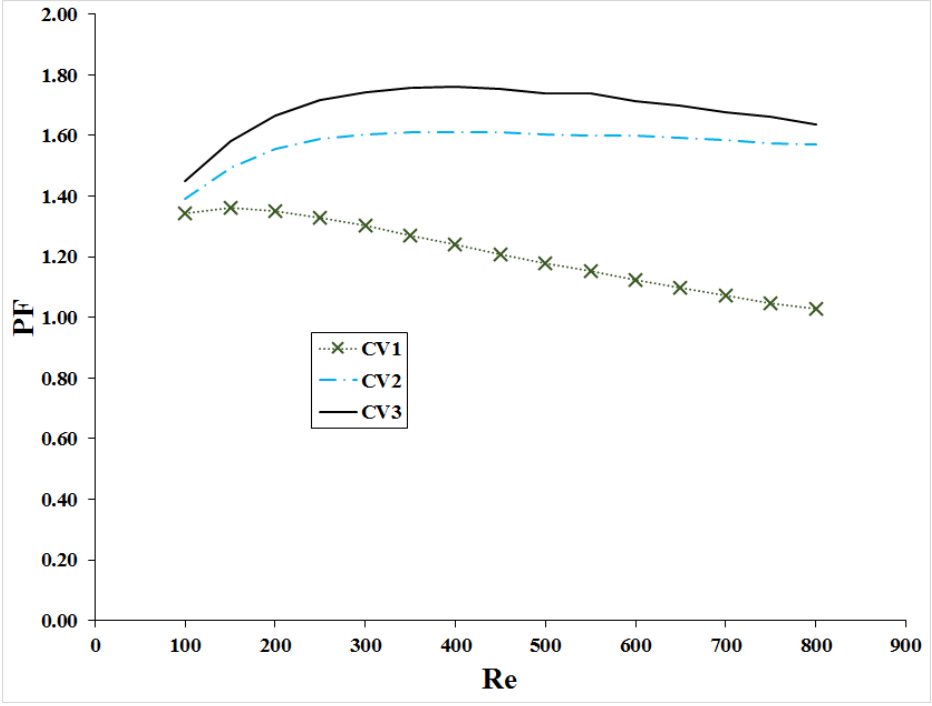

Fig. 7. Performance factor of all designs for the Re number of 100 to 800

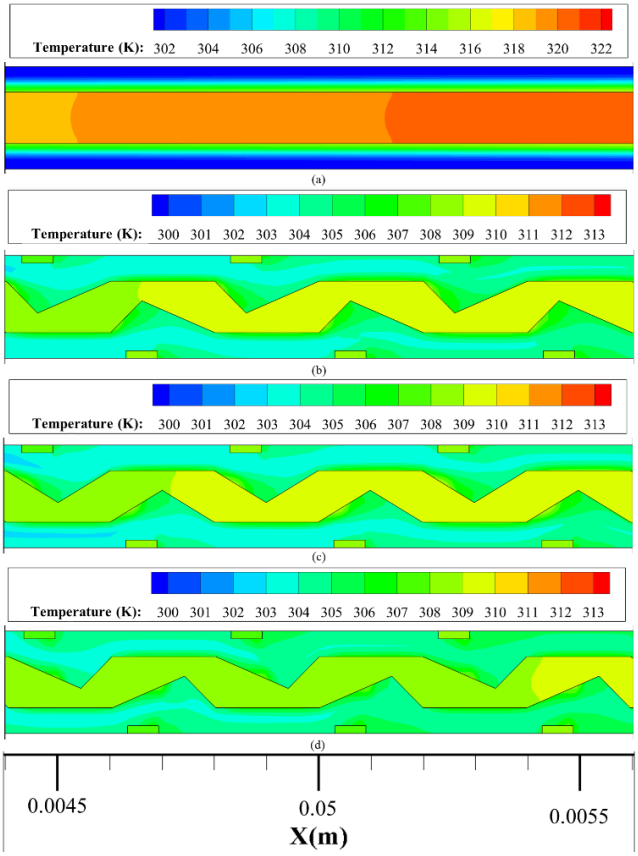

Fig. 8. Temperature distribution for Re number of 350 on x-y plane at z = 0.25mm (a) Conventional channel design (CR MCHS) (b) Cavity 1 channel design, CV1 (c) Cavity 2 channel design, CV2 (d) Cavity 3 channel design, CV3

4. Conclusion

Fluid flow and heat transfer characteristic in a hybrid microchannel heat sink with the triangular cavity and rectangular rib was studied numerically. Three different shapes of the triangular cavity were analysed based on friction factor ratio, (f/f_o), Nusselt number ratio, (Nu/Nu_o) and performance factor, Pf . For a more in-depth investigation, velocity and temperature distribution analysis were also conducted. The main findings are summarized as follows:

I. For an economic microchannel heat sink, CV1 design was the best triangular cavity design which had the lowest pressure drop that contributes to the less pumping power consumption compared to CV2 and CV3 designs. However, the CV1 design obtained the lowest heat transfer performance.

II. Among all the designs, CV3 design was the optimum design that can fulfil the thermal and economic management whereby it can provide high heat transfer rate with minimal pressure drop penalty. The optimum Performance Factor, PF, achieved by CV3 pitch location was 1.76 at Re number of 350.

III. The CV3 design was very effective at the lower Re number, which means the design is very suitable for the technology that requires less pumping power consumption.

IV. Location of vortex flow that generated in the cavity and at the downstream of rib plays the central role to increase the disturbance and degree of flow mixing, which contributes to heat transfer performance enhancement. The parallel vortex flow has changed the fluid flow structure in the CV3 design by increasing the chaotic advection.

V. The optimum operating condition of fluid velocity is very important to prevent a high-velocity gradient between vortex flows and main flow which affects the thermal resistance in the hybrid microchannel heat sink (TC-RR MCHS).

Acknowledgement

Authors wish to thanks Universiti Teknologi Malaysia for supporting this research activity under Takasago grant (R.K130000.7343.4B472)

References

[1] Tummala, Rao R. "Fundamentals of microsystems packaging." (2001): 190-193.

[2] Naqiuddin, Nor Haziq, Lip Huat Saw, Ming Chian Yew, Farazila Yusof, Hiew Mun Poon, Zuansi Cai, and Hui San Thiam. "Numerical investigation for optimizing segmented micro-channel heat sink by Taguchi-Grey method." *Applied Energy* 222 (2018): 437-450..
https://doi.org/10.1016/j.apenergy.2018.03.186

[3] Tuckerman, David B., and Roger Fabian W. Pease. "High-performance heat sinking for VLSI." *IEEE Electron device letters* 2, no. 5 (1981): 126-129.
https://doi.org/10.1109/EDL.1981.25367

[4] Wan Mohd Arif Aziz Japar, Nor Azwadi Che Sidik, Siti Rahmah Aid, Yutaka Asako, and Tan Lit Ken. "A Comprehensive Review on Numerical and Experimental Study of Nanofluid Performance in Microchannel Heatsink (MCHS)." *Journal of Advanced Research in Fluid Mechanics and Thermal Sciences* 45, no. 1 (2018): 165-176.

[5] Ansari, Danish, and Kwang-Yong Kim. "Hotspot thermal management using a microchannel-pinfin hybrid heat sink." *International Journal of Thermal Sciences* 134 (2018): 27-39.
https://doi.org/10.1016/j.ijthermalsci.2018.07.043

[6] Rui-jin Wang, Jia-wei Wang, Bei-qi Lijin, and Ze-fei Zhu. "Parameterization investigation on the microchannel heat sink with slant rectangular ribs by numerical simulation." *Applied Thermal Engineering* 133 (2018): 428-438.
https://doi.org/10.1016/j.applthermaleng.2018.01.021

[7] Yunfei Yan, Hongyu Yan, Siyou Yin, Li Zhang, and Lixian Li. "Single/multi-objective optimizations on hydraulic and thermal management in micro-channel heat sink with bionic Y-shaped fractal network by genetic algorithm coupled with numerical simulation." *International Journal of Heat and Mass Transfer* 129 (2019): 468-479.
https://doi.org/10.1016/j.ijheatmasstransfer.2018.09.120

[8] NM Noh, A Fazeli, and NA Che Sidik. "Numerical simulation of nanofluids for cooling efficiency in microchannel heat sink." *Journal of Advanced Research in Fluid Mechanics and Thermal Sciences* 4, no. 1 (2014): 13-23.

[9] SB Abubakar, NA Che Sidik. "Numerical prediction of laminar nanofluid flow in rectangular microchannel heat sink." *Journal of Advanced Research in Fluid Mechanics and Thermal Sciences* 7, no. 1 (2015): 29-38.

[10] Soo Weng Beng, and Wan Mohd Arif Aziz Japar. "Numerical analysis of heat and fluid flow in microchannel heat sink with triangular cavities." *Journal of Advanced research in fluid mechanics and thermal sciences* 34, no. 1 (2017): 1-8.

[11] Jia-Wei Zuo, Kok-Cheong Wong, and Hoon Kiat Ng. "The Thermal Performance of Three-Layered Microchannel Heat Sink with Tapered Channel Profile." *Journal of Advanced Research in Fluid Mechanics and Thermal Sciences* 56, no. 1 (2019): 147-156.

[12] Ihsan Ali Ghani, Natrah Kamaruzaman, and Nor Azwadi Che Sidik. "Heat transfer augmentation in a microchannel heat sink with sinusoidal cavities and rectangular ribs." *International Journal of Heat and Mass Transfer* 108 (2017): 1969-1981.
https://doi.org/10.1016/j.ijheatmasstransfer.2017.01.046

[13] YF Li, GD Xia, DD Ma, YT Jia, and J Wang. "Characteristics of laminar flow and heat transfer in microchannel heat sink with triangular cavities and rectangular ribs." *International Journal of Heat and Mass Transfer* 98 (2016): 17-28.
https://doi.org/10.1016/j.ijheatmasstransfer.2016.03.022

[14] Yifan Li, Guodong Xia, Yuting Jia, Dandan Ma, Bo Cai, and Jun Wang. "Effect of geometric configuration on the laminar flow and heat transfer in microchannel heat sinks with cavities and fins." *Numerical Heat Transfer, Part A: Applications* 71, no. 5 (2017): 528-546. https://doi.org/10.1080/10407782.2016.1277940

[15] Wan Mohd Arif Aziz Japar, Nor Azwadi Che Sidik, and Shabudin Mat. "A comprehensive study on heat transfer enhancement in microchannel heat sink with secondary channel." *International Communications in Heat and Mass Transfer* 99 (2018): 62-81. https://doi.org/10.1016/j.icheatmasstransfer.2018.10.005

[16] Wan Mohd Arif Aziz Japar and Nor Azwadi Che Sidik. *The effectiveness of secondary channel on the performance of hybrid microchannel heat sink at low pumping power*. in *IOP Conference Series: Materials Science and Engineering*. 2019. IOP Publishing. https://doi.org/10.1088/1757-899X/469/1/012032

[17] Richard J Phillips. "Microchannel heat sinks." *Advances in Thermal Modeling of Electronic Components* (1990)

[18] Ramesh K Shah and Alexander Louis London, *Laminar flow forced convection heat transfer and flow friction in straight and curved ducts-a summary of analytical solutions*. 1971, Stanford Univ CA Dept of Mechanical Engineering.

[19] Chang-Liang Han, Jing-Jie Ren, Wen-Ping Dong, and Ming-Shu Bi. "Numerical investigation of supercritical LNG convective heat transfer in a horizontal serpentine tube." *Cryogenics* 78 (2016): 1-13. https://doi.org/10.1016/j.cryogenics.2016.05.005

[20] Yi-Xin Hua, Ya-Zhou Wang, and Hua Meng. "A numerical study of supercritical forced convective heat transfer of n-heptane inside a horizontal miniature tube." *The Journal of Supercritical Fluids* 52, no. 1 (2010): 36-46. https://doi.org/10.1016/j.supflu.2009.12.003

[21] Ya-Zhou Wang, Yi-Xin Hua, and Hua Meng. "Numerical studies of supercritical turbulent convective heat transfer of cryogenic-propellant methane." *Journal of Thermophysics and Heat Transfer* 24, no. 3 (2010): 490-500. https://doi.org/10.2514/1.46769